Inorg. Chem. **2008**, *47*, 11382−11390

Reactivity of a Sterically Hindered Fe(II) Thiolate Dimer with Amines and Hydrazines

Michael J. Zdilla,[†] Atul K. Verma,[†] and Sonny C. Lee*[,‡]

Department of Chemistry, Princeton University, Princeton, New Jersey 08544, and Department of Chemistry, University of Waterloo, Waterloo, Ontario, Canada N2L 3G1

Received July 21, 2008

The sterically hindered Fe(II) thiolate dimer $Fe_2(\mu\text{-STriph})_2(STriph)_2$ (**1**; $[STriph]^- = 2,4,6$-triphenylbenzenethiolate) reacts with primary amines ($^t BuNH_2$, aniline) and N_2H_4 to form the structurally characterized addition complexes $Fe(STriph)_2(NH_2{}^tBu)_2$, $Fe_2(\mu\text{-STriph})_2(STriph)_2(NH_2Ph)_2$, and $Fe_2(\mu\text{-}\eta^1{:}\eta^1\text{-}N_2H_4)_2(N_2H_4)_4(STriph)_4$ in high yield. Chemical and NMR spectroscopic evidence indicate that the binding of these nitrogen donors is labile in solution and multispecies equilibria are likely. With arylhydrazines, **1** catalytically disproportionates 1,2-diphenylhydrazine to aniline and azobenzene, and it rearranges 1-methyl-1,2-diarylhydrazines to give, after treatment with alumina, mononuclear, trigonal bipyramidal Fe(III) complexes of composition $Fe(ISQ)_2(STriph)$, where $[ISQ]^-$ denotes an appropriately substituted bidentate *o*-diiminobenzosemiquinonate ligand. Complex **1** shows no reaction with hindered 1,2-dialkylhydrazines (isopropyl or *tert*-butyl) or tetrasubstituted 1,2-dimethyl-1,2-diphenylhydrazine.

Introduction

The binding and transformation of substrates by nitrogenases,[1] the metalloenzymes responsible for biological nitrogen fixation, is poorly understood at the molecular level.[2] Recent progress on this subject, however, has been significant and has yielded the first observations of long-sought enzyme intermediates during substrate reduction.[3] These advances rely on the combination of site-directed mutagenesis, flash-quench trapping, and EPR methods and have been employed effectively on a number of substrates. Of particular interest here is the substrate hydrazine (N_2H_4), for which an intermediate can be trapped and studied using a Mo-dependent nitrogenase protein mutated specifically to enlarge a reaction pocket at, and disrupt proton transfer to, the active site.[4−6] The N_2H_4-derived species was shown by electron nuclear double resonance (ENDOR) spectroscopy to be bound[6] to the FeMo-cofactor,[7,8] the $[MoFe_7S_9X]$ (X = 2p element) cluster believed to be the substrate reduction site in the Mo-dependent nitrogenases; from the side chain positions of the mutated amino acids, the site of binding was inferred to occur at an Fe−S face of the cluster[4] and, by extrapolation, at one or more iron centers. Chemically significant details regarding the nitrogenous ligand (e.g., identity, protonation and oxidation levels, binding mode and location in the cofactor cluster) are unavailable at present.

In this context, the study of iron-hydrazine interactions in small molecule complexes is useful in delineating intrinsic properties relevant to the interpretation of biophysical and biochemical results.[9] (In this report, hydrazine refers to the

* To whom correspondence should be addressed. E-mail: sclee@uwaterloo.ca.
† Princeton University.
‡ University of Waterloo.

(1) (a) Christiansen, J.; Dean, D. R.; Seefeldt, L. C. *Annu. Rev. Plant Physiol. Plant Mol. Biol.* **2001**, *52*, 269. (b) Burgess, B. K.; Lowe, D. L. *Chem. Rev.* **1996**, *96*, 2983. (c) Eady, R. R. *Chem. Rev.* **1996**, *96*, 3013.
(2) (a) Seefeldt, L. C.; Dance, I. G.; Dean, D. R. *Biochemistry* **2004**, *43*, 1401. (b) Igarashi, R. Y.; Seefeldt, L. C. *Crit. Rev. Biochem. Mol. Biol.* **2003**, *38*, 351.
(3) (a) Barney, B. M.; Lee, H.-I.; Dos Santos, P. C.; Hoffman, B. M.; Dean, D. R.; Seefeldt, L. C. *Dalton Trans.* **2006**, 2277. (b) Dos Santos, P. C.; Igarashi, R. Y.; Lee, H.-I.; Hoffman, B. M.; Seefeldt, L. C.; Dean, D. R. *Acc. Chem. Res.* **2005**, *38*, 208.
(4) Barney, B. M.; Igarashi, R. Y.; Dos Santos, P. C.; Dean, D. R.; Seefeldt, L. C. *J. Biol. Chem.* **2004**, *279*, 53621.
(5) Barney, B. M.; Yang, T.-C.; Igarashi, R. Y.; Dos Santos, P. C.; Laryukhin, M.; Lee, H.-I.; Hoffman, B. M.; Dean, D. R.; Seefeldt, L. C. *J. Am. Chem. Soc.* **2005**, *127*, 14960.
(6) Barney, B. M.; Laryukhin, M.; Igarashi, R. Y.; Lee, H.-I.; Dos Santos, P. C.; Yang, T.-C.; Hoffman, B. M.; Dean, D. R.; Seefeldt, L. C. *Biochemistry* **2005**, *44*, 8030.
(7) Einsle, O.; Tezcan, F. A.; Andrade, S.; Schmid, B.; Yoshida, M.; Howard, J. B.; Rees, D. C. *Science* **2002**, *297*, 1696.
(8) (a) Smith, B. E. *Adv. Inorg. Chem.* **1999**, *47*, 160. (b) Burgess, B. K. *Chem. Rev.* **1990**, *90*, 1377.
(9) For a recent example, see: Lees, N. S.; McNaughton, R. L.; Gregory, W. V.; Holland, P. L.; Hoffman, B. M. *J. Am. Chem. Soc.* **2008**, *130*, 546.

10.1021/ic801349y CCC: $40.75
Published on Web 11/01/2008

general chemical class unless specified explicitly or by context as the N_2H_4 molecule.) Indeed, much of existing iron-hydrazine chemistry, almost entirely predating the detection of N_2H_4-derived nitrogenase intermediates, has been inspired by the chemistry of biological nitrogen fixation. Of the limited set of structurally characterized iron-hydrazine species,[10−13] we note the extensive work of the Sellmann laboratory on 6-coordinate Fe(II) complexes with mixed bis(thiolate)/bis(thioether)/(amine or pyridine) pentadentate ancillary ligation[11] and 5-coordinate Fe(III) complexes with 1,2-benzendithiolate ligands.[12] Recent progress in this area includes the characterization of hydrazine and hydrazide adducts with mononuclear and sulfide-bridged dinuclear hindered β-diketiminate Fe(II) species[13a,b] and of an η^2 binding mode for N_2H_4 in a cationic Fe(II) polyphosphine complex.[13c] The reactivity of hydrazines with iron species has attracted similar attention. Parent hydrazine (N_2H_4) can be oxidized by dioxygen to ligated diazene (N_2H_2) in Fe(II) bis(thiolate)/bis(thioether)/(amine or phosphine) complexes,[14] while N−N bond reduction in hydrazines and hydrazides has been found in β-diketiminate and polyphosphine systems.[13] In our own work, we have demonstrated diarylhydrazine reduction by reactive Fe(II) amide thiolate complexes to form iron-imide heterocubane clusters,[15] and this has provided one impetus for our general exploration of the cluster chemistry of iron and nitrogen anions.[16]

In this report, we investigate the reactivity of hydrazines and, for comparison, amines with the homoleptic ferrous dimer, $Fe_2(\mu\text{-STriph})_2(STriph)_2$ (**1**; $[STriph]^- = 2,4,6$-triphenylbenzenethiolate), of Ruhlandt−Senge and Power.[17] The hindered thiolate ligation in complex **1** provides low-coordinate, high-spin Fe(II) centers in a constrained sulfur-anion environment that resists uncontrolled oligomerization/polymerization by thiolate bridging.[18] As such, these metal centers potentially simulate fundamental aspects of the reactive sulfide-ligated iron sites proposed to exist during nitrogenase substrate turnover.[2,19]

Scheme 1

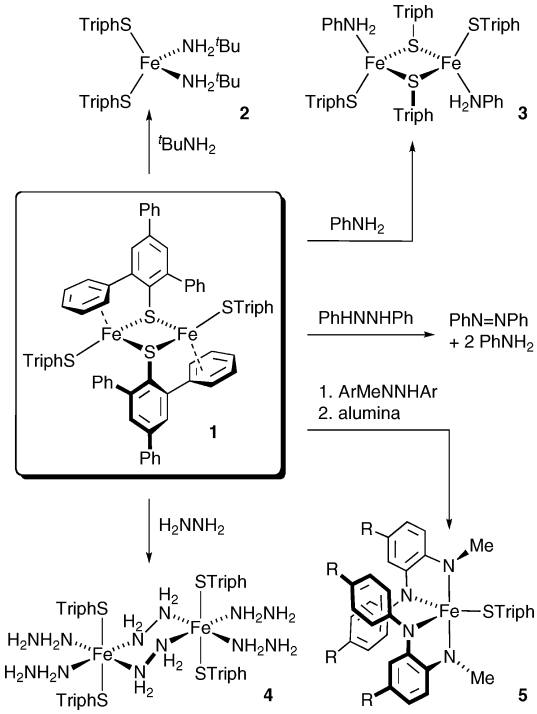

Results and Discussion

$Fe_2(\mu\text{-STriph})_2(STriph)_2$ (1). Complex **1** and its isostructural selenolate homologue[20] have received attention in previous studies primarily for their low-coordinate iron centers.[17,20−22] In the solid state, **1** adopts the centrosymmetric structure depicted in Scheme 1.[17] The environment at iron can be described as intermediate between 3- and 4-coordinate, with three strongly bound ligands (one terminal and two bridging thiolates) and a long, presumably weak, fourth interaction[18,22] with the π-face of an *o*-Ph ring on a bridging $[STriph]^-$ ligand (closest Fe−C contact: 2.53 Å); the metal geometry is discernibly pyramidalized toward this weak interaction. To our knowledge, there are no prior published reports of solution properties or chemical reactivity involving complex **1**.

To assist in solution studies, we investigated the ^{1}H NMR behavior of **1** in noncoordinating solvents. In C_6D_6 solution at 25 °C, complex **1** exhibits a characteristic ^{1}H NMR spectrum (Figure 1) dispersed by the paramagnetism of the high-spin metal centers across a range of about 55 ppm. This spectrum is insufficient to support a geometry assignment, as the number of signals (15 observed) and their intensities do not immediately correspond to any obvious molecular symmetry. Additional measurements at elevated temperatures, in an alternate solvent ($CDCl_3$), and using ^{1}H COSY were needed to relate the spectral signature to a solution structure. The data are organized and assigned in Table 1, with the assignment rationale provided as Supporting Infor-

(10) (a) Kumar, N. R. S.; Nethaji, M.; Patil, K. C. *Polyhedron* **1991**, *10*, 365. (b) Goedken, V. L.; Peng, S.-M.; Molin-Norris, J.; Park, Y.-a. *J. Am. Chem. Soc.* **1976**, *98*, 8391.
(11) (a) Sellmann, D.; Shaban, S. Y.; Heinemann, F. W. *Eur. J. Inorg. Chem.* **2004**, 4591. (b) Sellmann, D.; Blum, N.; Heinemann, F. W. *Z. Naturforsch.* **2001**, *56b*, 581. (c) Sellmann, D.; Soglowek, W.; Knoch, F.; Ritter, G.; Dengler, J. *Inorg. Chem.* **1992**, *31*, 3711.
(12) (a) Sellmann, D.; Friedrich, H.; Knoch, F. *Z. Naturforsch.* **1994**, *49b*, 660. (b) Sellmann, D.; Kreutzer, P.; Huttner, G.; Frank, A. *Z. Naturforsch.* **1978**, *33b*, 1341.
(13) (a) Vela, J.; Stoian, S.; Flaschenriem, C. J.; Münck, E.; Holland, P. L. *J. Am. Chem. Soc.* **2004**, *126*, 4522. (b) Smith, J. M.; Lachicotte, R. J.; Holland, P. J. *J. Am. Chem. Soc.* **2003**, *125*, 15752. (c) Crossland, J. L.; Zakharov, L. N.; Tyler, D. R. *Inorg. Chem.* **2007**, *46*, 10476.
(14) (a) Sellmann, D.; Friedrich, H.; Knoch, F.; Moll, M. *Z. Naturforsch.* **1993**, *48b*, 76. (b) Sellmann, D.; Soglowek, W.; Knoch, F.; Moll, M. *Angew. Chem., Int. Ed. Engl.* **1989**, *28*, 1271.
(15) Verma, A. K.; Lee, S. C. *J. Am. Chem. Soc.* **1999**, *121*, 10838.
(16) Lee, S. C.; Holm, R. H. *Chem. Rev.* **2004**, *104*, 1135.
(17) Ruhlandt-Senge, K.; Power, P. P. *Bull. Soc. Chim. Fr.* **1992**, *129*, 594.
(18) Nguyen, T.; Panda, A.; Olmstead, M. M.; Richards, A. F.; Stender, M.; Brynda, M.; Power, P. P. *J. Am. Chem. Soc.* **2005**, *127*, 8545.
(19) The utility of hindered thiolate ligands of this type in nitrogenase analogue chemistry is demonstrated in the recent preparation of topological analogues to the nitrogenase clusters: Ohki, Y.; Ikagawa, Y.; Tatsumi, K. *J. Am. Chem. Soc.* **2007**, *129*, 10457.
(20) (a) Hauptmann, R.; Kliss, R.; Henkel, G. *Angew. Chem., Int. Ed.* **1999**, *38*, 377. (b) Hauptmann, R.; Kliss, R.; Schneider, J.; Henkel, G. *Z. Anorg. Allg. Chem.* **1998**, *624*, 1927.
(21) MacDonnell, F. M.; Ruhlandt-Senge, K.; Ellison, J. J.; Holm, R. H.; Power, P. P. *Inorg. Chem.* **1995**, *34*, 1815.
(22) Evans, D. J.; Hughes, D. L.; Silver, J. *Inorg. Chem.* **1997**, *36*, 747.

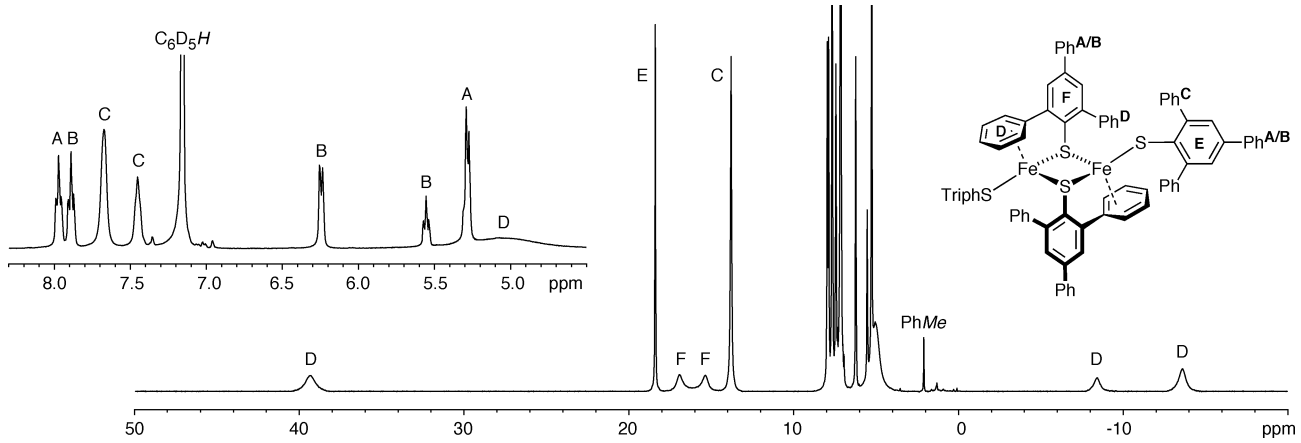

Figure 1. ^{1}H NMR spectrum of $Fe_2(\mu\text{-STriph})_2(STriph)_2$ (**1**; C_6D_6, 500 MHz, 295 K), with expansion of the 4.5−8.3 ppm region and labeling scheme (insets). Residual C_6D_5H and toluene (Ph*Me*) solvent signals are indicated explicitly.

Table 1. ^{1}H NMR Data for $Fe_2(\mu\text{-STriph})_2(STriph)_2$ (**1**)

assignment[a]	δ, ppm[b,c,d]	^{1}H−^{1}H COSY[e]
p-Ph (A)		
o,p-H	5.28 (m, 6H)[f]	*m*-H (A)
m-H	7.98 (pt, 4H)	*o,p*-H(A)
p-Ph (B)		
o-H	6.24 (d, 4H)	*m*-H (B)
m-H	7.90 (pt, 4H)	*o,p*-H(B)
p-H	5.55 (t, 2H)	*m*-H (B)
o-Ph, terminal STriph (C)		
o-H	13.82 (8H)	*m*-H (C)
m-H	7.68 (8H)	*o,p*-H(C)
p-H	7.46 (4H)	*m*-H (C)
o-Ph, μ-STriph (D)	−13.6 (br, 4H), −8.3 (v br, 2H), 5.0 (v br, ca. 10H),[g] 39.2 (v br, 4H)	
-$SC_6H_2Ph_3$, terminal STriph (E)	18.42 (4H)	
-$SC_6H_2Ph_3$, μ-STriph (F)	15.4 (v br, 2H),[h] 16.9 (v br, 2H)[h]	

[a] Phenyl rings are labeled in Figure 1. [b] C_6D_6 solution, 22 °C. [c] In parentheses: multiplicity (where observed), integrated intensity. [d] Abbreviations: d, doublet; pt, pseudotriplet; m, multiplet; br, broad; v br, very broad. [e] Signal correlations are indicated where observed. [f] The overlapping multiplet at 5.28 ppm resolves to two signals at 5.25 (pt, 2H, *p-H*) and 5.31 (d, 4H, *o-H*) ppm at 60 °C. [g] The very broad feature at 5.0 ppm is replaced by two signals at 5.0 (v br, 6H) and 5.3 (v br, 4H) ppm in $CDCl_3$ at 22 °C. [h] The two signals coalesce to a single resonance at 40 °C.

Table 2. Solution Spectroscopic Data for Fe-STriph Complexes[a]

	electronic absorption:[b] λ, nm (ε_M, L·mol^{-1}·cm^{-1})	^{1}H NMR:[c] δ, ppm
$Fe_2(STriph)_4$ (**1**)	250 (104,800), 290 (60,000)	see Table 1
$Fe(STriph)_2(NH_2{}^tBu)_2$ (**2**)	255 (90,000), 305 (45,000), 335 (35,000)[d]	−0.28 (2H), 0.48 (1H), 7.2 (v br), 8.65 (2H), 10.82 (4H), 11.27 (2H), 11.9 (br, 4H), 30.3 (2H)
$Fe_2(STriph)_4(NH_2Ph)_2$ (**3**)	355 (6000)[d]	0.27 (2H), 0.74 (1H), 5.47(br), 5.82 (s, excess amine), 6.17 (t, excess amine), 8.87 (2H), 9.69 (2H), 9.76 (4H), 13.6 (4H), 31.66 (2H)
$Fe_2(N_2H_4)_6(STriph)_4$ (**4**)	250 (102,000), 330 (40,500)	1.44 (2H), 1.82 (3H), 3.69 (1H), 6.50 (s), 6.87 (br), 7.14 (br), 9.95 (s), 10.0 (v br), 29.53 (br, 2H)
$Fe(STriph)(N\text{-Me-ISQ}^H)_2$ (**5a**)	245 (55,000), 285 (32,000), 350 (6600), 460 (4200), 550 (7500), 745 (2400)	not observed

[a] These solution data cannot be definitively associated with fixed solid state structures because of ligand lability; see text for details. [b] THF solution, 22 °C. [c] C_6D_6 solution (CD_2Cl_2 for **4**), 22 °C. [d] Generated in situ by addition of 15 equiv of $^tBuNH_2$ and 100 equiv of $PhNH_2$ to 0.54 and 0.054 mM solutions of **1**, respectively.

mation. Although an absolutely certain signal assignment is not possible even with the additional data and is probably unattainable without ligand derivatization, our qualified assignment is fully consistent with the retention of the centrosymmetric solid state structure in benzene and chloroform solution, with terminal thiolates that are unconstrained and bridging thiolates that show restricted C−S bond rotation and differentiated *o*-Ph groups on the observational timescales.

Reactivity Studies. The reaction chemistry of complex **1** as investigated in this work is summarized in Scheme 1. Spectroscopic data (electronic absorption and ^{1}H NMR) for the reaction products are compiled in Table 2. As noted below, the nitrogen donors are labile in these systems, and the reported solution spectra do not necessarily correspond to the species observed in the solid state. The optical spectra are dominated by strong, presumably sulfur-based charge transfer transitions in the UV region, with generally weak features in the visible range; a plot of the superimposed electronic absorption spectra is available in Supporting Information. The NMR data are analyzed together in a separate discussion of solution behavior. The solid state

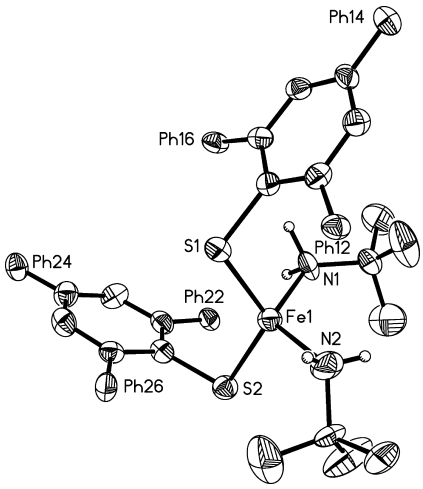

Figure 2. Structure of $Fe(STriph)_2(NH_2tBu)_2$ (**2**·0.5PhMe) with thermal ellipsoids (50% probability level) for non-hydrogen atoms and selected atom labels; N-bound hydrogens, placed at idealized positions, are also shown. For clarity, only the ipso carbon atoms, designated as "Ph", are depicted for the pendant phenyl groups of $[STriph]^-$ ligands.

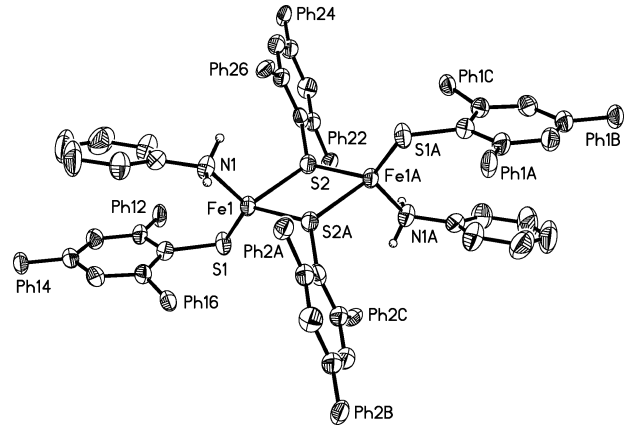

Figure 3. Structure of $Fe_2(\mu\text{-}STriph)_2(STriph)_2(NH_2Ph)_2$ (**3**·$2CH_2Cl_2$) with thermal ellipsoids (50% probability level) for non-hydrogen atoms and selected atom labels; N-bound hydrogens, placed at idealized positions, are also shown. Atoms designated as "Ph" are the ipso carbon atoms of the pendant phenyl groups of the $[STriph]^-$ ligands, which are otherwise omitted for clarity, and atoms with labels ending in "A" are generated by crystallographic inversion symmetry.

Table 3. Selected Interatomic Distances (Å) and Angles (deg) for $Fe(STriph)_2(NH_2tBu)_2$·0.5PhMe (**2**·0.5PhMe)

Fe1−N1	2.128(6)	Fe1−N2	2.132(7)
Fe1−S1	2.324(2)	Fe1−S2	2.317(2)
N1−Fe1−N2	119.7(3)	S1−Fe1−S2	124.60(8)
S1−Fe1−N1	102.6(2)	S1−Fe1−N2	100.2(3)
S2−Fe1−N1	101.6(2)	S2−Fe1−N2	109.6(2)

Table 4. Selected Interatomic distances (Å) and Angles (deg) for $Fe_2(\mu\text{-}STriph)_2(STriph)_2(NH_2Ph)_2$·$2CH_2Cl_2$ (**3**·$2CH_2Cl_2$)

Fe1−N1	2.110(4)	Fe1−S2	2.286(2)
Fe1−S1	2.364(2)	Fe1−S1A	2.375(2)
Fe1···Fe1A	3.688(2)	S1···S1A	2.976(3)
N1−Fe1−S1	113.76(14)	N1−Fe1−S1A	94.91(13)
N1−Fe1−S2	126.45(13)	S1−Fe1−S1A	77.79(7)
S2−Fe1−S1	101.68(7)	S2−Fe1−S1A	132.17(6)
Fe1−S1−Fe1A	102.21(7)		

structures and magnetic properties (where relevant) of individual compounds are presented specifically in the sections that follow.

1. Reactions with Amines, N_2H_4, and Alkylhydrazines. The treatment of red solutions of complex **1** with primary amines (^{t}BuNH$_2$ or aniline) or N_2H_4 gives yellow solutions, from which yellow ligand addition products ($Fe(STriph)_2(NH_2{}^t Bu)_2$, **2**; $Fe_2(\mu\text{-}STriph)_2(STriph)_2(NH_2Ph)_2$, **3**; or $Fe_2(\mu\text{-}\eta^1\text{:}\eta^1\text{-}N_2H_4)_2(N_2H_4)_4(STriph)_4$, **4**) can be crystallized in high (>80%) yields (Scheme 1). The lability of the introduced ligand complicates the solution behavior (vide infra) and necessitates the use of excess nitrogen donor (N-donor) for optimal preparative yields.

Reactions were also attempted with representative symmetric dialkylhydrazines. Neither 1,2-diisopropylhydrazine nor 1,2-di-*tert*-butylhydrazine showed any signs of reactivity with **1**, due, most likely, to the steric demands imposed by the *N*,*N*′-substituents. In contrast, reaction with 1,2-diethylhydrazine gives a solution color change to yellow that is similar to those observed for complexes **2**−**4** and is therefore taken to indicate ligand binding. The ^{1}H NMR spectrum of this system resembles the spectra of **2**−**4**, although the signals were broader and weaker in intensity; all attempts to isolate a well-defined product from this reaction were unsuccessful.

2. Structures of Amine and N_2H_4 Complexes. The three N-donor addition complexes **2**−**4** were identified by single crystal X-ray diffraction analyses. Each complex presents a different solid state structure, as shown in Figures 2−4.

For the reaction of **1** with ^{t}BuNH$_2$, a mixture of radiating acicular aggregates and isolated plates are obtained from the crystallization system. These two habits correspond to pseudopolymorphs of **2**, with the needles triclinic with one-half toluene lattice solvate per iron and the plate-like crystals orthorhombic with one toluene solvate per iron. As the structure of the complex is equivalent in both lattices, only the better-determined triclinic form is presented here, with details of the orthorhombic structure available as Supporting Information. Complex **2** (Figure 2, Table 3) is a mononuclear pseudotetrahedral coordination complex, consisting of an Fe(II) center ligated by two monoanionic $[STriph]^-$ ligands and two neutral ^{t}BuNH$_2$ ligands. The Fe−N bond lengths (2.13 Å) are similar to the shortest distances found for tetrahedral Fe(II)-(neutral amine) contacts, which have occurred previously only in the form of tertiary amine chelates.[23] The steric demands of the hindered thiolate ligands expand the S−Fe−S angle to 125°.

Complex **3** is a direct, bis(aniline) adduct of dinuclear **1** (Figure 3, Table 4), where aniline ligands bind at coordination sites formerly occupied by the weakly interacting *o*-Ph groups of the bridging $[STriph]^-$ ligands. The trans disposition of terminal ligands in **1** is retained in **3**, and both structures exhibit crystallographically imposed inversion symmetry.[17] Relative to the intermediate 3- to 4-coordinate metal geometry found in **1**,[17] the metal centers in **3** are clearly recognizable as 4-coordinate pseudotetrahedral, with compression of the (μ-S)-Fe-(μ-S) angle (78° vs 97° in **1**) and

(23) (a) Lorber, C.; Choukroun, R.; Costes, J.-P.; Donnadieu, B. *C. R. Chim.* **2002**, *5*, 251. (b) Komuro, T.; Kawaguchi, H.; Tatsumi, K. *Inorg. Chem.* **2002**, *41*, 5083. (c) Handley, D. A.; Hitchcock, P. B.; Lee, T. H.; Leigh, G. J. *Inorg. Chim. Acta* **2001**, *314*, 14. (d) Calderazzo, F.; Englert, U.; Pampaloni, G.; Vanni, E. *C. R. Acad. Sci., Ser. IIc: Chim.* **1999**, *2*, 311.

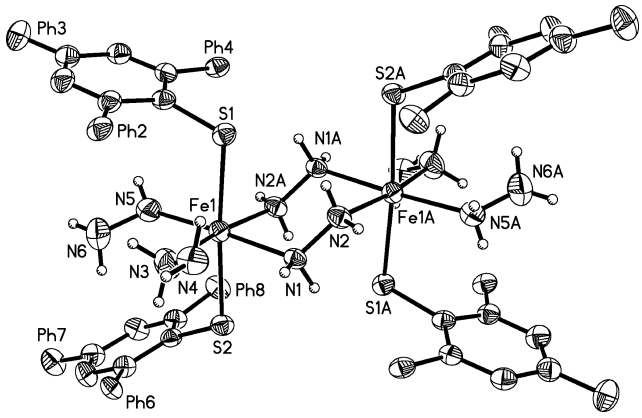

Figure 4. Structure of $Fe_2(\mu\text{-}\eta^1\text{:}\eta^1\text{-}N_2H_4)_2(N_2H_4)_4(STriph)_4$ ($\mathbf{4}\cdot N_2H_4\cdot 1.5THF$) with thermal ellipsoids (50% probability level) for non-hydrogen atoms and selected atom labels. Hydrazine hydrogens are also shown; these were located and refined with the exception of hydrogens belonging to a disordered hydrazine ligand (N3−N4), which were placed at idealized positions. Atoms designated as "Ph" are the ipso carbon atoms of the pendant phenyl groups of the [STriph]- ligands, which are otherwise omitted for clarity, and atoms with labels ending in "A" are generated by crystallographic inversion symmetry. Only one of two independent centrosymmetric dimers is presented.

Table 5. Selected Mean Interatomic Distances (Å) and Angles (deg) for $Fe_2(\mu\text{-}N_2H_4)_2(N_2H_4)_4(STriph)_4\cdot N_2H_4\cdot 1.5THF$ ($\mathbf{4}\cdot N_2H_4\cdot 1.5THF$)[a,b]

Fe−N_b	2.225(2)	Fe−N_t	2.215(15)
Fe−S	2.492(3)	Fe···Fe	4.33(2)
N_b−N_b	1.4535(7)	N_t−N	1.432(10)[c]
N_b−Fe−N_b	86.5(5)	N_t−Fe−N_t	95.7(9)
cis N_b−Fe−N_t	89(3)	trans N_b−Fe−N_t	174(3)
N_b−Fe−S	89(3)	N_t−Fe-S	91(2)
S−Fe−S	174.2(8)	Fe−N_b−N_b	118(3)
Fe−N_t-N_t	114.8(9)		

[a] Tabulated entries are the arithmetic means of all structural metrics of the type indicated, including both independent half-dimers; the uncertainties represent the standard deviations from the means and are, in almost all cases, greater than the estimated standard deviations for the individual metrics. [b] N_b and N_t refer to donor nitrogen atoms on bridging and terminal hydrazines, respectively. [c] The N3−N4 distance is not included in the mean because of disorder at N4.

corresponding expansion of the Fe−(μ-S)−Fe angle (102° vs 83°). The changes in ligand and geometry increase slightly the Fe−S bond distances in **3** relative to **1** (Fe−S(terminal), 2.286(2) vs 2.262(3) Å; Fe−(μ-S), 2.364(2) and 2.375(2) vs 2.337(3) and 2.378(3) Å). Arylamines are uncommon ligands, and only three other structurally characterized examples of monodentate arylamine ligation at iron exist in the literature, all at the Fe(II) oxidation level.[24] The Fe−NH_2Ar bond distance in **3** (2.11 Å) is shorter than those previously reported (2.18, 2.25, 2.28 Å) because of differences in coordination numbers and steric constraints, but it is comparable to the tetrahedral Fe(II)−($NH_2{}^t$Bu) contact observed in complex **2**.

The crystal structure of **4** (Figure 4, Table 5) reveals two independent half-dimers in the asymmetric unit, with crystallographic inversion symmetry relating each half-dimer to the full dimeric structure. The dinuclear core in these dimers consists of a pair of octahedral iron centers cis-bridged by two η^1:η^1-N_2H_4 ligands to form a six-membered ring in a chair conformation. This motif is precedented in infinite chain structures $[M(\mu\text{-}\eta^1\text{:}\eta^1\text{-}N_2H_4)_2X_2]_n$ (M = divalent 3d transition metal ion),[25] but is new to discrete molecular systems; only one other molecular complex is known where two N_2H_4 bridges span two metal sites, and this occurs in the presence of a third, disulfide ligand bridge.[26] Two trans axial $[STriph]^-$ ligands and two terminal end-bound cis equatorial N_2H_4 ligands complete the coordination sphere at each iron. The sterically encumbered $[STriph]^-$ ligand appears to prevent the catenation found previously in $[M(N_2H_4)_2X_2]$ systems, while the reduced steric demand of N_2H_4 ligation allows for the octahedral metal stereochemistry in **4** rather than the tetrahedral geometry found in complexes **2** and **3**. The two independent complexes in the cell are structurally equivalent except for internal disorder; one contains two symmetry-related disordered terminal hydrazines, while the other shows two symmetry-related disordered phenyl groups. The N−N bond lengths for the bridging hydrazines in **4** are indistinguishable from those measured for free N_2H_4 (1.45−1.46 Å)[27] or in the $[M(\mu\text{-}\eta^1\text{:}\eta^1\text{-}N_2H_4)_2X_2]_n$ systems,[25] whereas the N−N distances for the terminal hydrazines are slightly shorter; the latter observation is most likely an artifact of minor disorder or increased motion associated with the unligated nitrogen atoms. The Fe−N distances are all at approximately 2.2 Å and are consistent with neutral N_2H_4 ligation at an octahedral high-spin Fe(II) center.[10a,11c,28] The Fe−S(terminal) bonds are lengthened to 2.5 Å in **4** relative to compounds **2** and **3** (2.3 Å) due presumably to the increased coordination number; the steric bulk of the Triph group in the octahedral environment and the trans disposition of the thiolate donors may also add to the Fe−S distance. The presence of high-spin ($S = 2$) Fe(II) sites was verified by magnetic susceptibility measurements (4−260 K), which showed temperature-dependent effective magnetic moments (μ_{eff}) in the range of 5.4 to 5.7 μ_B per iron;[29] plots of magnetic moment and inverse susceptibility versus temperature are provided as Supporting Information.

3. Solution Behavior of Amine and N_2H_4 Complexes. The formation of complexes **2**−**4** can be described by the simple reaction stoichiometries given in eqs 1−3.

$$Fe_2(\mu\text{-STriph})_2(STriph)_2 + 4{}^t\text{BuNH}_2 \rightleftharpoons 2Fe(STriph)_2(NH_2{}^t\text{Bu})_2 \quad (1)$$

$$Fe_2(\mu\text{-STriph})_2(STriph)_2 + 2PhNH_2 \rightleftharpoons Fe_2(\mu\text{-STriph})_2(STriph)_2(NH_2Ph)_2 \quad (2)$$

(24) (a) Carson, E. C.; Lippard, S. J. *Inorg. Chem.* **2006**, *45*, 828. (b) Eckert, N. A.; Smith, J. M.; Lachicotte, R. J.; Holland, P. L. *Inorg. Chem.* **2004**, *43*, 3306. (c) Dickman, M. H. *Acta Crystallogr.* **2000**, *C56*, 58.

(25) (a) Braibanti, A.; Bigliardi, G.; Canali Padovani, R.; Dallavalle, F. *Gazz. Chim. Ital.* **1965**, *95*, 1212. (b) Ferrari, A.; Braibanti, A.; Bigliardi, G.; Lanfredi, A. M. *Acta Crystallogr.* **1965**, *19*, 548. (c) Ferrari, A.; Braibanti, A.; Bigliardi, G.; Dallavalle, F. *Z. Kristallogr.* **1963**, *119*, 284. (d) Ferrari, A.; Braibanti, A.; Bigliardi, G. *Acta Crystallogr.* **1963**, *16*, 498.

(26) Matsumoto, K.; Uemura, H.; Kawano, M. *Chem. Lett.* **1994**, 1215.

(27) (a) Liminga, R.; Olovsson, I. *Acta Crystallogr.* **1964**, *17*, 1523. (b) Collin, R. L.; Lipscomb, W. N. *Acta Crystallogr.* **1951**, *4*, 10.

(28) Although no magnetic measurements were reported, we assume from the ligand set that the $[Fe(N_2H_4)_2(OH_2)_2Cl_2]^{2-}$ complex reported in ref 10a is high-spin.

(29) Figgis, B. N.; Lewis, J.; Mabbs, F. E.; Webb, G. A. *J. Chem. Soc., A* **1967**, 442.

$$Fe_2(\mu\text{-STriph})_2(STriph)_2 + 6N_2H_4 \rightleftharpoons Fe_2(\mu\text{-}\eta^1\text{:}\eta^1\text{-}N_2H_4)_2(N_2H_4)_4(STriph)_4 \quad (3)$$

The actual chemistry in solution is complicated by ligand lability and the relatively weak binding associated with nonchelate N-donors at high spin Fe(II). For example, the reaction system of **1** and excess ^{t}BuNH$_2$ in toluene evinces a yellow solution color indicative of ligand binding and yields crystalline **2** upon introduction of *n*-pentane and cooling; this system, however, is in reversible equilibrium inasmuch as the direct removal of solvent in vacuo (rather than pentane-induced slow crystallization) results in the complete loss of amine and the recovery of starting complex **1**. Similarly, aniline adduct **3** reverts completely to **1** when dissolved in C_6D_6 at millimolar concentrations as determined by ^{1}H NMR analysis, although the spectral signature of **1** under these conditions shows just one coalesced *m*-H Ph^F signal for the bridging [STriph]$^-$ ligand, rather than the two separated Ph^F resonances that exist for solutions of pure **1** at room temperature (Figure 1, Table 1). This last finding suggests that transient aniline ligation facilitates the interconversion of these inequivalent *m*-H positions in **1**, perhaps by disrupting the weak iron-arene π-interaction, thereby lowering the barrier to C−S bond rotation at the bridging thiolate. We note that this coalescence can be achieved thermally at +40 °C, indicating that the chemical exchange process is readily accessible even in the absence of aniline (see Supporting Information).

In C_6D_6 solution at room temperature, the ^{t}BuNH$_2$ complex **2** and the hydrazine complex **4** display closely related ^{1}H NMR spectra (Figure 5) despite their very different solid state structures. Although aniline complex **3** transforms to **1** under these conditions (demonstrating the weaker binding ability of the arylamine donor), a spectrum similar to those of **2** and **4** can be obtained when **1** is treated with 30 equiv of aniline (Figure 3). In all three cases, the spectra show isotropically shifted, relaxation broadened resonances consistent with one type of [STriph]$^-$ ligand, symmetry-averaged across all rotational degrees of freedom; amine/hydrazine associated signals are also evident. The positions of the thiolate resonances are characteristic and fall within shared chemical shift regions for all three samples (Table 2). In total, these observations suggest a common predominant solution structure throughout.

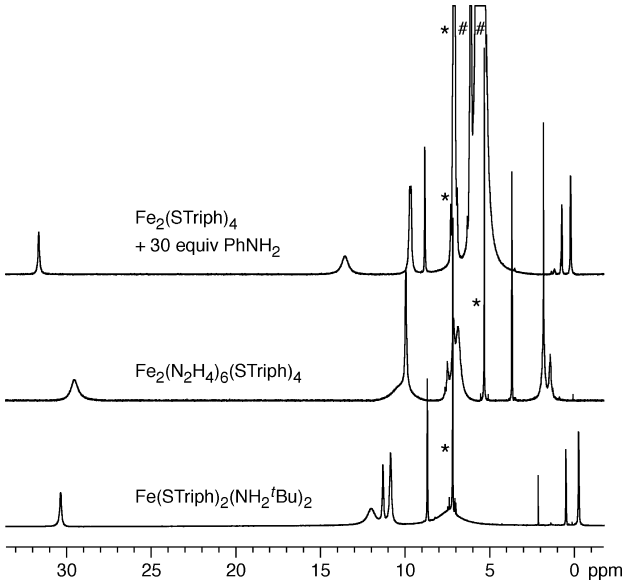

Figure 5. Comparative ^{1}H NMR spectra (295 K) of complexes **2** (bottom; 400 MHz, C_6D_6) and **4** (center; 400 MHz, CD_2Cl_2), and of complex **1** treated with 30 equiv of $PhNH_2$ (top; C_6D_6, 500 MHz). Residual protiosolvent and excess (free) aniline signals are indicated by * and #, respectively.

Mononuclear complex **2** possesses the simplest structure type that can directly account for the [STriph]$^-$ features in the NMR spectra. As supporting evidence, we compare the positions of the two downfield resonances reported[30] for $[Fe(STriph)_4]^{2-}$ at 31 and 15 ppm to similar signals that occur in our spectra in the 29−32 and 10−14 ppm ranges. Although the $[Fe(STriph)_4]^{2-}$ complex was the subject of only a brief report and has not been structurally characterized, we can also consider the related, well-understood mononuclear $[Fe(SPh)_4]^{2-}$ complex,[31] the *m*-H resonance of which appears at about 22 ppm. On the basis of these data and on relative integrated intensities, it is reasonable to assign the signals in the 29−32 ppm region to the *m*-H on the thiolate arene ($SC_6\mathit{H}_2Ph_3$) of a [STriph]$^-$ ligand in a mononuclear, pseudotetrahedral Fe(II) complex. The lability of the coordination environment and the available evidence, however, render the assignment of solution structure conjectural at present.

Given the chemical and spectroscopic observations, it seems likely that facile, multispecies equilibria are accessible in solution for these reaction systems, with the solid state structures of **2**−**4** representing points on the speciation pathways. Dinuclear aniline adduct **3** and mononuclear bis(^{t}BuNH$_2$) complex **2** would constitute intermediate and end point species, respectively, for amine addition to complex **1**. Similarly, hydrazine complex **4** would be an intermediate form in a speciation manifold made more complex by the low steric demand of N_2H_4 and the existence of bridging ligation modes.

4. Reactions with Arylhydrazines. A 3 mM benzene solution of **1** will completely convert 6 equiv of 1,2-diphenylhydrazine (PhHNNHPh) to aniline and azobenzene (PhN=NPh) in a 2:1 ratio over the course of 30 min. This transformation corresponds to a catalytic disproportionation process per eq 4. The starting complex is the only other species evident in this system and is recoverable in quantity in the form of aniline adduct **3**.

$$2PhHNNHPh \rightarrow 2PhNH_2 + PhN{=}NPh \quad (4)$$

In an effort to direct the chemistry away from disproportionation, reactions with *N*-substituted 1,2-diarylhydrazines were explored. The tetrasubstituted 1,2-dimethyl-1,2-diphenylhydrazine (PhMeNNMePh) is inert to reaction with complex **1** under our reaction conditions. By contrast, addition of the trisubstituted 1-methyl-1,2-diphenylhydrazine (PhMeNNHPh) to a red benzene solution of **1** gives a deep

(30) Sun, W.-Y.; Ueyama, N.; Nakamura, A. *Spectrosc. Lett.* **1998**, *38*, 871.
(31) Hagen, K. S.; Reynolds, J. G.; Holm, R. H. *J. Am. Chem. Soc.* **1981**, *103*, 4054.

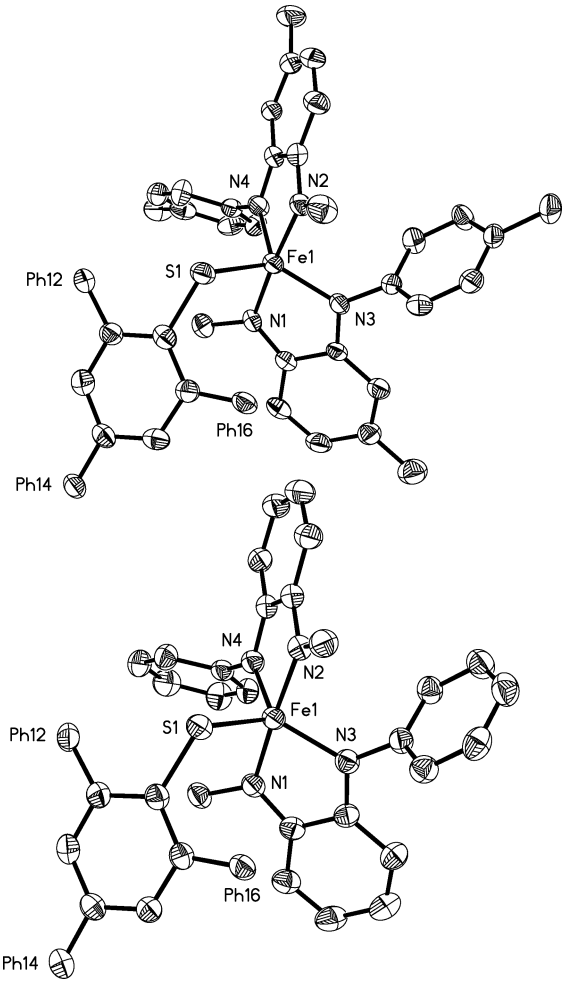

Figure 6. Structures of Fe(STriph)(*N*-R′-ISQ^{R})$_2$ (R′ = Me, R = H: **5a**·C_6H_6, bottom; R′ = R = Me: **5b**·Et_2O, top) with thermal ellipsoids (50% probability level) for non-hydrogen atoms and selected atom labels. For the pendant phenyl groups of [STriph]$^-$ ligands, only the ipso carbon atoms, designated as "Ph", are depicted; hydrogen atoms are not shown.

blue solution after several hours. Complex **3** is observed as a minor product component by ^{1}H NMR spectroscopy and can be isolated by evaporation of the benzene solvent and extraction of the dry residue with pentane; its presence demonstrates that reductive cleavage of the hydrazine still occurs to a limited extent (<5% yield) despite the removal of the disproportionation pathway. No other species could be identified or isolated directly from this reaction mixture.

A tractable complex can be obtained in quantity from this system by treating the foregoing blue benzene solution with activated alumina, resulting in a purple solution from which the purple crystalline product **5a** can be obtained in about 30% yield. The remaining reaction mass, which is adsorbed on the alumina, can be freed by extraction with acetonitrile to afford blue solutions, but we were unable to obtain any well-defined materials from this fraction. The reaction of **1** with 1-methyl-1,2-di(*p*-tolyl)hydrazine ((*p*-Tol)MeNNH(*p*-Tol)) proceeds similarly to yield purple crystals of complex **5b**. Neither **5a** nor **5b** nor any of the blue solutions display ^{1}H NMR features other than minor contaminant signals.

Table 6. Selected Interatomic Distances (Å) and Angles (deg) for Fe(STriph)(*N*-Me-ISQ^{H})$_2$·C_6H_6 (**5a**·C_6H_6) and Fe(STriph)(*N*-Me-ISQ^{Me})$_2$·Et_2O (**5b**·Et_2O)[a]

	5a	5b
Fe1−N1/2	1.895(2)/1.901(2)	1.899(4)/1.899(4)
Fe1−N3/4	1.922(2)/1.924(2)	1.909(4)/1.921(4)
Fe1−S1	2.2684(10)	2.2543(14)
N1−Fe1−N3/4	81.86(10)/98.38(10)	81.8(2)/99.7(2)
N2−Fe1−N3/4	95.57(10)/81.88(10)	94.2(2)/81.9(2)
N1/3−Fe1−N2/4	176.88(11)/129.72(10)	176.0(2)/125.50(15)
S1−Fe1−N1/2	96.84(8)/85.94(8)	95.88(11)/86.92(12)
S1−Fe1−N3/4	118.90(8)/111.02(8)	123.76(11)/110.36(12)

[a] Divided entries refer to separate atoms and their associated metrics in the order given, e.g., N1/3−Fe1−N2/4 denotes two angles, N1−Fe1−N2 and N3−Fe1−N4, respectively.

Because of the lack of obvious spectroscopic signatures,[32] we were unable to determine whether alumina is simply an adsorbant in our protocol, or whether it plays an active chemical role in the formation of **5a** and **5b**; PhMeNNHPh by itself is stable in the presence of activated alumina.

Crystallographic analyses reveal that products **5a** and **5b** are analogous mononuclear 5-coordinate complexes of formulation Fe(STriph)(*N*-R′-ISQ^{R})$_2$ (**5a**, R′ = Me, R = H; **5b**, R′ = R = Me; Figure 6, Table 6). The bidentate ISQ ligand nucleus is a derivative of *o*-phenylenediamine absent one hydrogen at each nitrogen, and it can exist at three different oxidation levels. Its assignment here as the monoanionic π-radical diiminobenzosemiquinonate and the inference of the Fe(III) oxidation state derive from correspondences in compound type and structural metrics to the closely related [FeL(*N*-H-ISQ^{H})$_2$]^z complexes (z = 0, 1+; L = neutral or monoanionic ligand), the electronic properties of which were the focus of a recent, comprehensive analysis.[33] These previously reported 5-coordinate species are square pyramidal, with ligand L apical; the trigonality parameter τ[34] ranges from 0.00 to 0.37 in this set, with τ < 0.06 in 4 of the 6 reported complexes. By contrast, the iron centers in **5a** and **5b** possess trigonal bipyramidal (TBP) coordination geometries, with τ = 0.79 (**5a**) and 0.84 (**5b**) and the methylated nitrogens occupying axial positions. We ascribe the TBP geometry preference in the present complexes to the relief of the steric congestion associated with the bulky [STriph]$^-$ ligand and with the *N*-methylation of the ISQ chelate.

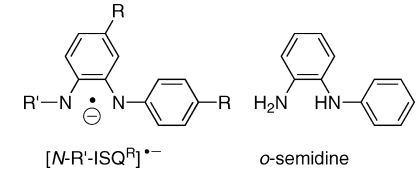

(32) In addition to their NMR silence, complexes **5a** and **5b** are EPR inactive, and their optical absorption bands are obscured (if present) by other intense, broad absorptions in the deep blue crude reaction solutions.

(33) Chłopek, K.; Bill, E.; Weyhermüller, T.; Wieghardt, K. *Inorg. Chem.* **2005**, *44*, 7087.

(34) $\tau = (\beta - \alpha)/60$, where β and α are the largest and next-largest interligand bond angles, respectively; τ = 0 for an ideal square pyramid and 1 for an ideal trigonal bipyramid: Addison, A. W.; Rao, T. N.; Reedijk, J.; van Rijn, J.; Verschoor, G. C. *J. Chem. Soc., Dalton Trans.* **1984**, 1349.

The role of complex **1** in the arylhydrazine transformations is unknown. These transformations have extensive organic precedent in the acid-catalyzed and thermal rearrangement chemistries of 1,2-diarylhydrazines, which give a variety of products depending on aryl group and reaction conditions (e.g., treatment with dilute HCl in aqueous/EtOH solution, or heating at 80−110 °C over the course of hours).[35] Setting aside differences in protonation and oxidation states, the formation of the ISQ moiety is structurally analogous to the rearrangement of 1,2-diphenylhydrazine to *o*-semidine. Likewise, disproportionation occurs frequently as an accompanying and sometimes dominant process in these chemistries. Metal-mediated variants of both reactions have also been reported in isolated instances.[36,37] The organic transformations have been studied in detail and their mechanisms explicated, whereas the metal-based examples have received much less attention and are largely undefined from a mechanistic perspective. In the present system, the function of complex **1** in the arylhydrazine transformations is obscured by spectroscopic and synthetic constraints. The available observations nevertheless indicate that arylhydrazines, which have been used by us[15] and others[13,38] in nitrogenase mimetic studies, present new, unanticipated complexities in metal-derived reactivity.

Conclusions

The chemistry of the sterically hindered, ferrous thiolate complex **1** with amines and hydrazines ranges from no reaction to simple ligand additions to major substrate rearrangements coupled with redox and protonation state changes. Two general findings of potential value in nitrogenase-related synthetic study and biochemical interpretation are emphasized:

1. For primary amines, N_2H_4, and alkyl-substituted hydrazines, N-donor ligation is the typical outcome in this hindered, low-coordinate iron system, steric factors permitting. There is no evidence of N−N bond activation for these hydrazines by Fe(II) in a simple thiolate environment under aprotic conditions. The coordination of N-donors leads to a variety of structures in the solid state that differ in bridging environment and coordination geometry, and N-donor lability likely gives rise to multispecies equilibria in solution. These results highlight the challenge in engineering well-defined, constrained reaction centers at high-spin iron using only thiolates as ancillary ligands.

2. 1,2-Diarylhydrazines and their derivatives exhibit complicated chemistry involving catalytic disproportionation and structural rearrangement. The present examples add to the list of iron-mediated aryl-nitrogen transformations, which also includes reductive N−N bond cleavage,[13a,15] N=N bond reductions (in the presence of a hydride source),[13b,38] stoichiometric disproportionation of coordinated diphenylhydrazide,[13b] and oxidative coupling of arylamines to azoarenes.[39] It is apparent from the diversity of reaction outcomes that the interaction of iron with aryl-nitrogen species is complex, incompletely understood, and open for further investigation.

Experimental Section

General Considerations. Previously described anaerobic synthetic and spectroscopic (^{1}H NMR, UV−vis) protocols[39] were used in the present study. Brockman grade I neutral alumina was activated by heating at 300 °C for 24 h under dynamic vacuum. C_6D_6 solvent was stored over either 4 Å molecular sieves or sodium−lead alloy (Aldrich) for at least 24 h prior to use. Magnetic measurements were made using a Quantum Design Model 6000 Physical Property Measurement System. Elemental analyses were performed by the Microanalysis Laboratory at the University of Illinois, Urbana/Champaign. $Fe_2(\mu\text{-STriph})_2(STriph)_2$ (**1**),[17] 1,2-diisopropylhydrazine,[40] 1,2-di-*t*-butylhydrazine,[41] 1,2-di-*p*-tolylhydrazine,[42] 1-methyl-1,2-diphenylhydrazine,[43] 1-methyl-1,2-di-*p*-tolylhydrazine,[43] and 1,2-dimethyl-1,2-diphenylhydrazine[43] were prepared by literature methods. 1,2-Diethylhydrazine was obtained from the commercially available dihydrochloride salt (Aldrich) by treatment with excess 40% aqueous KOH, followed by extraction with CH_2Cl_2, preliminary drying over KOH, and final distillation from CaH_2. All other chemicals were obtained (in anhydrous form, if available) from commercial sources.

$Fe(STriph)_2(NH_2{}^tBu)_2$ (2). Neat $^tBuNH_2$ (24 μL, 0.2 mmol, d = 0.696 g/mL) was added to a red-orange solution of **1** (50 mg, 0.034 mmol) in 3 mL of toluene, affording a solution color change from deep red-orange to yellow upon mixing (1 min). This solution was diluted to 12 mL with *n*-pentane and chilled to −30 °C for 3 d to give a yellow crystalline material, which was isolated and washed with *n*-pentane. Yield: 50 mg (83%). Anal. Calcd for $C_{56}H_{56}N_2S_2Fe\cdot 1/2\ C_7H_8$: C, 77.42; H, 6.55; N, 3.03. Found: C, 77.33; H, 6.57; N, 3.03.

$Fe_2(\mu\text{-STriph})_2(STriph)_2(NH_2Ph)_2$ (3). Neat $PhNH_2$ (18 μL, 0.2 mmol, d = 1.022 g/mL) was added to a red-orange solution of **1** (100 mg, 0.0684 mmol) in 2 mL of CH_2Cl_2, affording a solution color change from deep red-orange to orange-yellow upon mixing (1 min). Vapor diffusion of *n*-pentane into this solution at −30 °C for 1 week gave yellow crystalline material, which was isolated and washed with *n*-pentane (88 mg). The supernatant was diluted with 5 mL of *n*-pentane and held at −30 °C to obtain a second crop (11 mg). Total yield: 99 mg (0.060 mmol, 88%). Anal. Calcd for $C_{108}H_{82}N_2S_4Fe_2\cdot CH_2Cl_2$: C, 75.56; H, 4.89; N, 1.62. Found: C, 75.82; H, 4.78; N, 1.76.

(35) (a) Cox, R. A.; Buncel, E. In *The Chemistry of Hydrazo, Azo, and Azoxy Groups*; Patai, S., Ed.; Wiley: New York, 1997; Vol. *2*, Chapter 15. (b) Cox, R. A.; Buncel, E. In *The Chemistry of Hydrazo, Azo, and Azoxy Groups*; Patai, S., Ed.; Wiley: New York, 1975; Vol. *1*, Chapter 18.

(36) (a) Xia, A.; James, A. J.; Sharp, P. R. *Organometallics* **1999**, *18*, 451. (b) Davis, C. J.; Heaton, B. T.; Jacob, C. *J. Chem. Soc., Chem. Commun.* **1995**, 1177.

(37) (a) Blackmore, K. J.; Lal, N.; Ziller, J. W.; Heyduk, A. F. *J. Am. Chem. Soc.* **2008**, *130*, 2728. (b) Hoover, J. M.; DiPasquale, A.; Mayer, J. M.; Michael, F. E. *Organometallics* **2007**, *26*, 3297. (c) Nakajima, Y.; Suzuki, H. *Organometallics* **2005**, *24*, 1860. (d) Barkley, J. V.; Heaton, B. T.; Jacob, C.; Mageswaran, R.; Sampanthar, J. T. *J. Chem. Soc., Dalton Trans.* **1998**, 697. (e) Takei, I.; Dohki, K.; Kobayashi, K.; Suzuki, T.; Hidai, M. *Inorg. Chem.* **2005**, *44*, 3768. (f) Kuwata, S.; Mizobe, Y.; Hidai, M. *Inorg. Chem.* **1994**, *33*, 3619. (g) Hitchcock, P. B.; Hughes, D. L.; Maguire, M. J.; Marjani, K.; Richards, R. L. *J. Chem. Soc., Dalton Trans.* **1997**, 4747.

(38) Ohki, Y.; Takikawa, Y.; Hatanaka, T.; Tatsumi, K. *Organometallics* **2006**, *25*, 3111.

(39) Duncan, J. S.; Nazif, T. M.; Verma, A. K.; Lee, S. C. *Inorg. Chem.* **2003**, *42*, 1211.

(40) Ghali, N. I.; Venton, D. L.; Hung, S. C.; Le Breton, G. C. *J. Org. Chem.* **1981**, *46*, 5413.

(41) Stowell, J. C. *J. Org. Chem.* **1967**, *32*, 2360.

(42) Carlin, R. B.; Wich, G. S. *J. Am. Chem. Soc.* **1958**, *80*, 4023.

(43) Katritzky, A. R.; Wu, J.; Verin, S. V. *Synthesis* **1995**, 651.

Table 7. Crystallographic Data for $Fe(STriph)_2(NH_2{}^t Bu)_2 \cdot PhMe$ (**2**·0.5PhMe), $Fe_2(STriph)_4(NH_2Ph)_2 \cdot 2CH_2Cl_2$ (**3**·$2CH_2Cl_2$), $Fe_2(N_2H_4)_6(STriph)_4 \cdot N_2H_4 \cdot 1.5THF$ (**4**·N_2H_4·1.5THF), $Fe(STriph)(N\text{-Me-ISQ}^H)_2 \cdot C_6H_6$ (**5a**·C_6H_6), and $Fe(STriph)(N\text{-Me-ISQ}^{Me})_2 \cdot Et_2O$ (**5b**·Et_2O)[a]

	2·0.5PhMe	**3**·$2CH_2Cl_2$	**4**·N_2H_4·1.5THF	**5a**·C_6H_6	**5b**·Et_2O
formula	$C_{59.5}H_{60}FeN_2S_2$	$C_{112}H_{90}Cl_8Fe_2N_2S_4$	$C_{102}H_{108}Fe_2N_{14}O_{1.5}S_4$	$C_{56}H_{47}FeN_4S$	$C_{58}H_{59}FeN_4OS$
fw	923.07	1987.40	1793.96	863.89	916.00
space group	$P\bar{1}$ (No. 2)	$P\bar{1}$ (No. 2)	$P\bar{1}$ (No. 2)	$P2_1/c$ (No. 14)	$P2_1/c$ (No. 14)
Z	2	1	2	4	4
a, Å	11.188(2)	12.276(3)	13,5817(14)	11.363(2)	12.006(2)
b, Å	12.099(2)	12.791(3)	18.8132(15)	19.154(4)	20.159(4)
c, Å	19.913(4)	18.173(4)	19.608(2)	21.950(4)	20.486(4)
α, deg	104.66(3)	88.04(3)	68.624(5)		
β, deg	92.79(3)	74.45(3)	89.564(4)	112.67(3)	96.24(3)
γ, deg	95.16(3)	63.27(3)	83.087(5)		
V, (Å^3)	2590.1(9)	2442.9(9)	4627.9(8)	4408.3(15)	4929.2(17)
ρ_{calc}, g/cm^3	1.184	1.351	1.287	1.302	1.234
θ_{max}, deg	22.20	22.44	25.00	25.01	22.46
total data,[b] %	98.9	98.9	98.6	99.90	99.7
μ, mm^{-1}	0.410	0.427	0.461	0.433	0.392
R_1 (wR_2),[c] %	12.26 (16.27)	7.31 (16.68)	5.26 (12.10)	5.30 (13.85)	7.86 (14.77)
S[d]	1.273	1.071	1.027	1.044	1.192

[a] Data collected at $T = 200(2)$ K using Φ and ω scans with graphite-monochromatized Mo Kα radiation ($\lambda = 0.71073$ Å). [b] Percent completeness of (unique) data collection within the θ_{max} limit. [c] Calculated for $I > 2\sigma(I)$: $R_1 = \sum||F_o| - |F_c||/\sum|F_o|$, $wR_2 = \{\sum[w(F_o^2 - F_c^2)^2]/\sum[w(F_o^2)^2]\}^{1/2}$. [d] S = goodness of fit = $\{\sum[w(F_o^2 - F_c^2)^2]/(n - p)\}^{1/2}$, where n is the number of reflections and p is the number of parameters refined.

$Fe_2(\mu\text{-}\eta^1\text{:}\eta^1\text{-}N_2H_4)_2(N_2H_4)_4(STriph)_4$ (4). Compound **4** can be isolated by standard procedures similar to those employed for complexes **2** and **3**; recrystallization of the isolated material, however, invariably yielded poorly crystalline material, probably because of loss of labile hydrazine. The following protocol was developed to obtain highly crystalline **4** reliably and in quantity: Neat hydrazine (1.5 mL reservoir) was vapor diffused at room temperature into a red-orange solution of **1** (75 mg, 0.051 mmol) in 1.5 mL of THF. Yellow crystals of **4** appeared in limited quantity after 1−2 h, but redissolved over the course of 3 d to give a clear yellow solution. The reservoir was then replaced with *n*-pentane, which was allowed to vapor diffuse into the reaction solution at −30 °C. After 1 week, yellow crystals of **4** and white crystals of hydrazine were collected by filtration and washed with cold THF to remove the hydrazine (care must be taken to avoid melting the hydrazine, as liquid hydrazine dissolves **4**), leaving pure, crystalline **4**. Yield: 81 mg (86%). Anal. Calcd for $C_{96}H_{92}N_{12}S_4Fe_2 \cdot 1.5(C_4H_8O)$: C, 69.53; H, 5.95; N, 9.54. Found: C, 70.18; H, 6.00; N, 9.39.

Reactions with 1,2-dialkylhydrazines. Conditions similar to those for the preparation of complexes **2** and **3** were used. For example, neat 1,2-diethylhydrazine (44.5 μL, 0.41 mmol, $d = 0.809$ g/mL) was added to a deep red-orange solution of **1** (100 mg, 0.0684 mmol) in 3 mL of benzene to give a transparent yellow solution over the course of 15 min; all efforts to isolate a pure product from this reaction were unsuccessful. Test reactions employing more hindered 1,2-diisopropylhydrazine and 1,2-di-*t*-butylhydrazine did not produce color changes and showed no other sign of reaction.

$Fe(STriph)(N\text{-Me-ISQ}^H)_2$ (5a). A colorless benzene solution (10 mL) of 1-methyl-1,2-diphenylhydrazine (PhMeNNHPh, 109 mg, 0.550 mmol) was added with stirring to a red-orange suspension of **1** (200 mg, 0.137 mmol) in benzene (10 mL), resulting in a color change to blue-black over the course of 10 h. After 1 d, neutral alumina (7.5 g) was added and the mixture stirred for an additional 20 h to afford a color change to purple. The mixture was filtered to remove the alumina, and the purple filtrate evaporated to dryness in vacuo. The resulting solid was recrystallized from C_6H_6/*n*-pentane to give **5a** as purple crystals. Yield: 66 mg (31%). We were unable to obtain accurate elemental analyses because of persistent contamination by $(TriphS)_2$. The synthesis of $Fe(STriph)(N\text{-Me-ISQ}^{Me})_2$ (**5b**) proceeds similarly using 1-methyl-1,2-di-*p*-tolylhydrazine, with the final crystallization achieved using Et_2O/*n*-pentane at −30 °C.

X-ray Crystallography. Single crystals suitable for X-ray diffraction analysis were obtained from the following conditions: **2**·0.5PhMe and **2**·PhMe (two pseudopolymorphs) as yellow radiating acicular aggregates and yellow plates, respectively, from toluene/*n*-pentane vapor diffusion at −30 °C; **3**·$2CH_2Cl_2$ as yellow plates, from CH_2Cl_2/*n*-pentane vapor diffusion at −30 °C; **4**·N_2H_4·1.5THF as yellow parallelpipeds, directly from the preparative reaction system; **5a**·C_6H_6 as blue-black blocks, from C_6H_6/*n*-pentane vapor diffusion at 25 °C; **5b**·Et_2O as blue-black blocks, from Et_2O/*n*-pentane vapor diffusion at −30 °C.

General crystallographic procedures are detailed elsewhere.[44] ψ-scan absorption corrections were applied using the Siemens SHELXTL software suite,[45] and multiscan absorption corrections were applied using PLATON.[46] Appropriate disorder models and restraints were employed as needed, and SQUEEZE-BYPASS[47] (implemented in PLATON) was used to remove the electron density associated with disordered solvent in **2**·PhMe and **4**·N_2H_4·1.5THF. Essential crystallographic data for the compounds in this work are summarized in Table 7, with specific details for individual structure determinations available as Supporting Information.

Acknowledgment. This research was supported by the Arnold and Mabel Beckman Foundation (Beckman Young Investigator Award), the U.S. National Science Foundation (CAREER CHE-9984645), and NSERC. We thank Prof. R. Cava and Dr. T. Klimczuk (Princeton) for assistance with magnetochemical measurements.

Supporting Information Available: Crystallographic data and comparative UV−vis spectra for compounds **2**, **3**, **4**, **5a**, and **5b**; NMR spectroscopic assignment and COSY data for complex **1**; and magnetochemical data for complex **4**. This material is available free of charge via the Internet at http://pubs.acs.org.

IC801349Y

(44) Kayal, A.; Ducruet, A. F.; Lee, S. C. *Inorg. Chem.* **2000**, *39*, 3696.
(45) Sheldrick, G. M. *SHELXTL*, Version 5.04; Siemens Analytical X-ray Instruments: Madison, WI, 1996.
(46) Spek, A. L. *Acta Crystallogr., Sect. A: Found. Crystallogr.* **1990**, *46*, C34.
(47) Van der Sluis, P.; Spek, A. L. *Acta Crystallogr., Sect. A: Found. Crystallogr.* **1990**, *46*, 194.